

# High performance doubly clamped piezoresistive accelerometers by the outturn of electroplating

B. Anupama<sup>1</sup>

<sup>1</sup> Assistant Professor, Department of Electronics & Communication Engineering, MES College of Engineering, Kerala, India

\*\*\*

**Abstract** - MEMS accelerometers find application in various fields such as vibration monitoring, inertial guidance, seismology, micro-gravity measurement, etc. and demand for high performance accelerometer for various applications is increasing. Although several conversion mechanisms and physical processes are found useful for acceleration sensing, piezoresistive accelerometers are cost effective as compared to other sensing mechanisms. Performance improvement of quad beam accelerometer in terms of displacement sensitivity and rotational cross axis sensitivity are presented in this paper. The improvement is achieved by incorporating a thick layer of gold on top of the proof mass of the accelerometer structure. To reduce cross axis sensitivity, center of mass has to be closer to the plane of beams. This can be accomplished by depositing gold on top of proof mass. Addition of gold on top of proof mass allows use of reduced silicon proof mass thickness and improves real estate consumption due to sloping side wall. Here we use gold as the deposited layer on the proof mass. This is because the density of bulk gold (19.32 grams/cm<sup>3</sup>) is nearly eight times more than that of crystal silicon (2.33 g/cm<sup>3</sup>). Also it is chemically inert to most of the chemicals used in micromachining process. In the present work, three different accelerometer structures are considered for performance evaluation in terms of sensitivity, cross axis sensitivity, linearity and silicon real estate consumption. Parametric analysis is performed by using simple analytical models by varying geometrical dimensions of the various parts of accelerometer structures. Effect of electroplated gold layer on the performance characteristics of each structure is studied.

**Key Words:** Sensitivity, cross axis sensitivity, piezoresistive effect

## 1. INTRODUCTION

MEMS accelerometers find application in various fields such as vibration monitoring, inertial guidance, micro-gravity measurement, etc. Demand for high performance accelerometer for various applications is still increasing and it is essential to realize these sensors in a cost effective way. Research has been carried out to deploy accelerometers in new applications such as automobile pollution control systems [1,2]. Although several conversion mechanisms and physical processes are found useful for acceleration sensing, piezoresistive accelerometers are cost effective as compared to other sensing mechanisms [3-7]. The main advantage of piezoresistive accelerometers is the simplicity of their structure and fabrication process. Also they are less susceptible to parasitic capacitance and electromagnetic interference.

It is challenging to achieve simultaneously high sensitivity and low cross axis sensitivity in designing micro accelerometers. Moreover these devices show a high range of cross axis sensitivity which is a major issue principally for high performance applications. To overcome this drawback, a MEMS piezoresistive single axis accelerometers with electroplated gold layer atop proof mass to enhance the performance of the sensor has been developed [13]. However, only quad beam accelerometer structures with their beams oriented in single direction with fixed dimension was considered.

## 2. DEVICE DETAILS

Three different accelerometer structures are considered in the present study as shown in Fig-1. They consist of a thick proof mass supported by four thin flexures that are fixed to an outer supporting frame. The two opposite edges of the flexures are clamped by the frame and proof mass.

### 2.1 Structural configuration

In the structure shown in Fig-1 (a), all the four flexures are oriented along X - direction which is parallel to wafer

primary flat. In the structure shown in Fig-1 (b), (here after structure 2), the four flexures are located at the centre of the proof mass edges whereas the accelerometer structure shown in Fig-1 (c), (here after structure 3), the four flexures are shifted to the corners of the edges and oriented along both X and Y directions. Piezoresistors may be implanted on the maximum stress region at the fixed-ends of flexures to form Wheatstone bridge for signal pick-up.

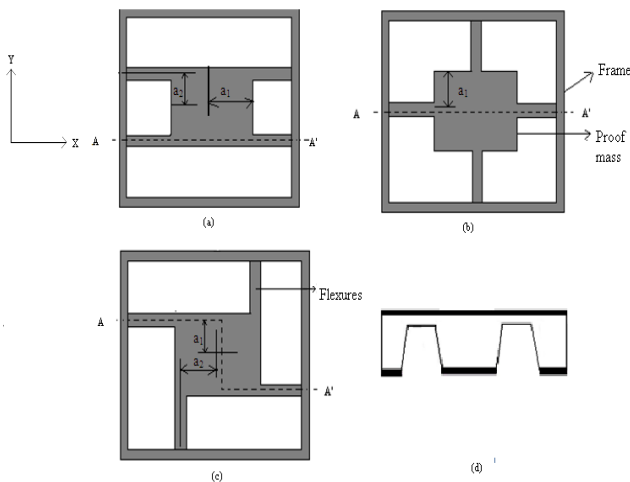


**Fig-1:**Four beam structures with beams located a) at the edges oriented to X axis (b) at the centre of the proof mass on all the edges (c) at the corners of the proof mass oriented to X and Y axes (d) Cross sectional view of the structure across AA'

Cantilever structures with single beam is not considered in the present study, because it is more sensitive to cross-axis accelerations along X and Y directions. Even though, cross axis response can be reduced by using two beam cantilever structure, only half-active Wheatstone bridge can be formed by using this structure.

## 2.2 Parametric equations

In an accelerometer structure, spring constant along a particular direction depends on the following parameters; (a) number of flexures (b) geometrical dimension of the flexures (c) position of the flexures. To achieve low cross axis sensitivity along a particular direction, spring constant should be high along that direction.

In the present study, for the fixed-fixed quad beam structure where all flexures are placed parallel to X-axis as shown in Fig-1 (a), equation of the spring constant along Z, X and Y axes can be written from [5], as

$$K_z = \frac{4Ew_b h_b^3}{l_b^3} \tag{1}$$

$$K_x = \frac{(l_b^2 + 3a_1 l_b + 3a_1^2)}{3} K_z \tag{2}$$

$$K_y = a_2^2 K_z \tag{3}$$

where E is the Young's Modulus, \$w\_b\$ is the width of the beam, \$l\_b\$ is the length of the beam, \$h\_b\$ is the thickness of the beam, \$a\_1\$ is the distance between the centre of proof mass and the proof mass edge along Y direction and \$a\_2\$ is the distance between the centre of flexure and proof mass along X direction as shown in Fig-1. \$K\_x\$, \$K\_y\$ and \$K\_z\$ represents the spring constant along X, Y and Z axes, respectively. Similar expressions are found for other multiple suspended beam configuration as in (1). The spring constant along Z axis for the other two configurations are the same. However, the spring constant along X and Y axes for these structures differ.

In the case of structure shown in Fig-1(b) the equation for the spring constant along X and Y axes are same and can be written from [5], as

$$K_x = K_y = \frac{(l_b^2 + 3a_1 l_b + 3a_1^2)}{6} K_z \tag{4}$$

For the structure with beams shifted away from the proof mass centre and aligned with the proof mass edges shown in Fig-1(c), the equation for the spring constants are given from [5], as

$$K_x = K_y = \frac{(l_b^2 + 3a_1 l_b + 3a_1^2 + 3a_2^2)}{6} K_z \tag{5}$$

The equation for rotation of proof mass around the X-axis (\$\theta\_x\$) for Y-axis acceleration for all the three structures can be written from [5], as

$$\theta_x = \frac{Ma_y Zc}{K_y} \tag{6}$$

where \$a\_y\$ is the acceleration along the Y axis, \$Zc\$ is distance between the center of mass (cg) of the proof mass and plane of the flexures and M is the mass of the proof mass. Similarly, the equation for rotation of proof mass around the Y-axis (\$\theta\_y\$) for X-axis acceleration in general can be written from [5], as

$$\theta_y = \frac{Ma_x Zc}{K_x} \tag{7}$$

where  $a_x$  is the acceleration along the X-axis.

The displacement of mass,  $\Delta_z$ , due to applied acceleration along z direction for all the three structures is given from [5], by

$$\Delta_z = \frac{Ma_z}{K_z} \tag{8}$$

where M is the mass of proof mass,  $a_z$  is the acceleration applied along z direction and  $K_z$  is the spring constant along z direction. It is clear from the (8) that the sensitivity is directly proportional to the mass of the proof mass. So as the mass of proof mass is increased by electroplating gold on top of it, the displacement increases and hence the sensitivity.

### 3. METHODOLOGY

The different parameters used for the parametric sensitivity analysis are the length of the beam, thickness of the beam and width of the beam for acceleration up to +1 g and for fixed proof mass dimensions. The analysis is done by varying one of the parameter and by fixing the other two parameters. Initially, the length of beam is varied from 400 $\mu\text{m}$  to 2000 $\mu\text{m}$  with width of the beam and thickness of the beam fixed to 250 $\mu\text{m}$  and 30 $\mu\text{m}$ , respectively. Subsequently, the width of the beam is varied from 50 $\mu\text{m}$  to 500 $\mu\text{m}$  in steps of 50 $\mu\text{m}$ , with the thickness of beam and length of the beam fixed to 30 $\mu\text{m}$  and 1200 $\mu\text{m}$ , respectively. By fixing the length of the beam to 1200 $\mu\text{m}$  and width of the beam to 250 $\mu\text{m}$  and by varying the thickness of the beam from 20 $\mu\text{m}$  to 60 $\mu\text{m}$ , the performance parameters in terms of prime axis displacement sensitivity and cross axis response are analyzed.

### 4. RESULTS AND DISCUSSION

To demonstrate the performance enhancement of an accelerometer, the material parameters are selected as  $E=1.69\text{GPa}$  and density of gold as  $19.28\text{kg/m}^3$ . As geometrical parameters, width of the beam and thickness of the beam are fixed to 250  $\mu\text{m}$  and 30  $\mu\text{m}$  respectively, and the length of the beam is varied there is an increase in displacement as shown in Fig-2. This increase in displacement is higher for the structure with electroplated gold.

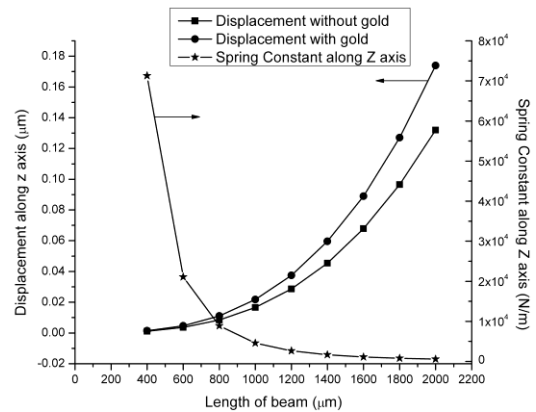


Fig -2 : Variation of displacement of proof mass and spring constant along Z axis with length of the beam

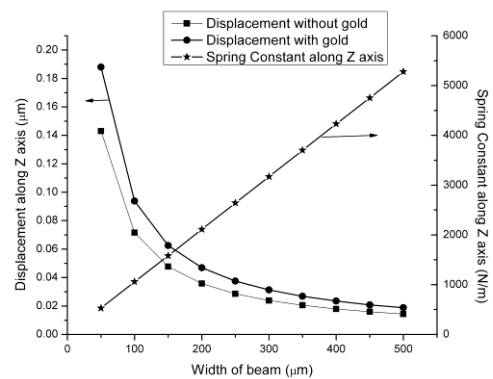


Fig-3: Variation of displacement of proof mass and spring constant along Z axis with width of the beam

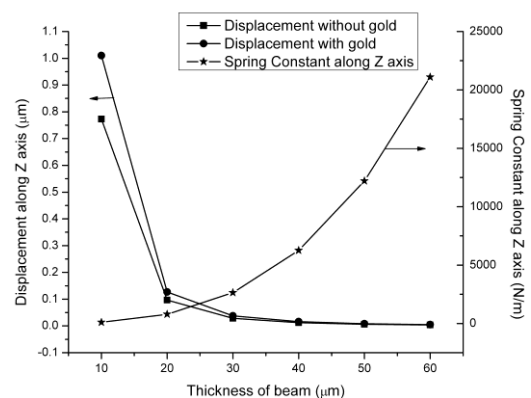
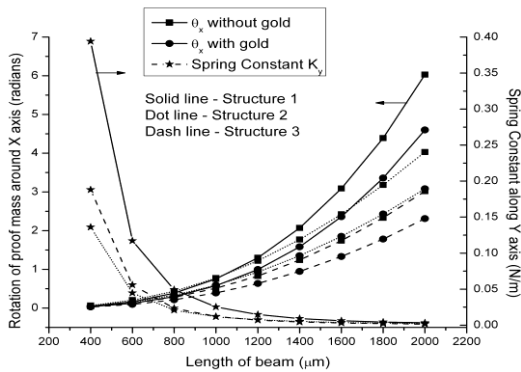


Fig -4 : Variation of displacement of proof mass and spring constant along Z axis with thickness of the beam

As the width of the beam is varied from 50 $\mu\text{m}$  to 500 $\mu\text{m}$ , it can be seen from the Fig-3 that there is a decrease in sensitivity and an increase in spring constant. But from the simulation it can be deduced that structure with electroplated gold has more sensitivity than the structure without electroplated gold. There is a constant percentage increase of around 23.9% in sensitivity for the structure with gold as the width of the beam is varied.

As the thickness of the beam is varied from 10µm to 60µm it can be seen from the Fig-4 that there is a decrease in sensitivity and an increase in spring constant. But from the simulation it can be deduced that structure with electroplated gold has more sensitivity than the structure without electroplated gold. There is a percentage increase from 23.46% to 23.68% in sensitivity for the structure with gold as the thickness of the beam is varied.



**Fig -5:** Variation of rotational cross axis sensitivity of proof mass and spring constant for Y axis acceleration with length of the beam

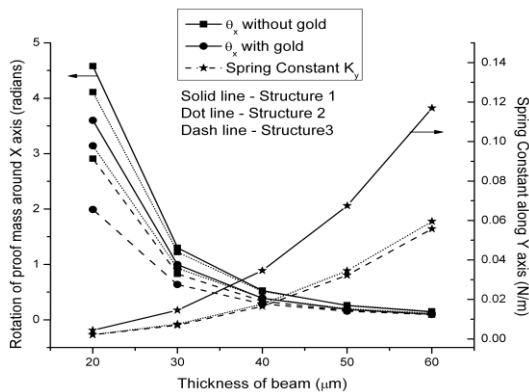


**Fig -6:** Variation of rotational cross axis sensitivity of proof mass and spring constant for Y axis acceleration with thickness of the beam

Fig- 5 shows the plot between rotation of proof mass around X axis and Spring Constant along Y axis for a variation in beam length. It can be seen that as the length of the beam is varied from 200µm to 2000µm it can be seen that there is a decrease in spring constant and an increase in rotational cross axis sensitivity. For the quad beam configuration 1 there is a percentage decrease in cross axis sensitivity from 23.65% to 23.71% for the structure with gold as the length of the beam is varied. For configuration 2 the simulation results shows that structure with electroplated gold has less cross axis sensitivity than the structure without gold. It is observed that there is a constant decrement in cross axis sensitivity around 23.58%. For quad beam configuration 3, as the length is

increased there is a decrease in spring constant from 86.07% to 21.94% for the structure with gold. Also it can be deduced that the increase in rotation is lesser for structure with electroplated gold and a percentage decrease in rotation from 23.49% to 23.54% is observed.

As the thickness of the beam is varied from 10µm to 60µm it can be seen from the Fig-6 that there is a decrease in rotational cross axis sensitivity and an increase in spring constant. But from the simulation it can be deduced that structure with electroplated gold has less cross axis sensitivity than the structure without electroplated gold. For quad beam configuration 1, there is a percentage decrement in cross axis sensitivity from 21.39% to 31.2% for the structure with electroplated gold as the thickness is increased. In the case of configuration 2, the percentage decrease in cross axis sensitivity for the structure with electroplated gold is observed to be a constant value of 23.63%. For configuration 3, there is a decrease in cross axis sensitivity which is lesser for structure with electroplated gold. The percentage reduction was observed to be varying from 23.49% to 31.6% for the structure with electroplated gold.

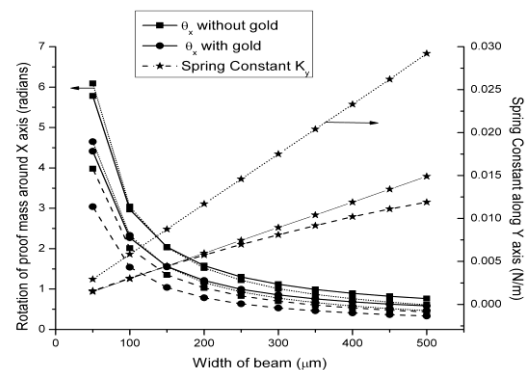


**Fig -7:** Variation of rotational cross axis sensitivity of proof and spring constant for Y axis acceleration with width of the beam

For quad beam configuration 1, when the width of the beam is increased from 50µm to 500µm, there is a decrease in rotation of proof mass around X axis as shown in Fig-7. It can be observed from the simulation results that the rotation is lesser for structure with electroplated gold. The percentage decrease observed is found to be varying from 23.7% to 23.56%. In the case of quad beam configuration where the beams are positioned at the centre on all edges of the proof mass, there is a constant percentage decrease of around 23.64% in cross axis sensitivity for the structure with gold as the width of the beam is varied. For the quad beam configuration 3, as the width of the beam is increased there is an increase in spring constant while a decrease in cross axis sensitivity is observed.

From all the previous simulation results it is clear that configuration 1 with beams positioned at the edges of the proof mass has got least cross axis sensitivity. So this structure is best in terms of rotational cross axis sensitivity around X axis. It is clear from Fig-8 that as the length of beam is increased from 200 $\mu\text{m}$  to 2000 $\mu\text{m}$  there is a decrease in cross axis sensitivity which is lesser for structure with electroplated gold. For multiple suspension beam configuration 1 there is a percentage decrease in cross axis sensitivity from 23.7% to 23.5% for the structure without gold. The simulation results shows that structure with electroplated gold has less cross axis sensitivity than the structure without gold for configuration 2. It is observed that there is a constant decrement in cross axis sensitivity around 23.58%. For quad beam configuration 3, as the length is increased there is a decrease in spring constant from 86.07% to 21.94% for the structure with gold. Also it can be deduced that the increase in rotation is lesser for structure with electroplated gold and a percentage decrease in rotation from 23.49% to 23.54% is observed.

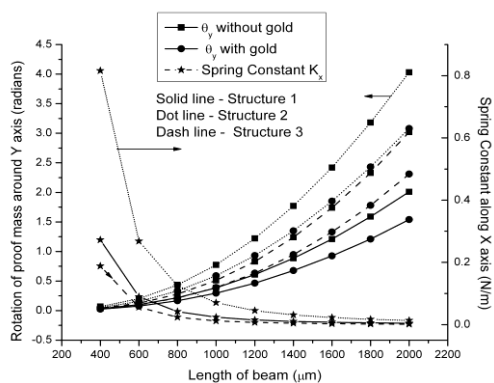


**Fig-8:** Variation of rotational cross axis sensitivity of proof mass and spring constant for X axis acceleration with length of the beam

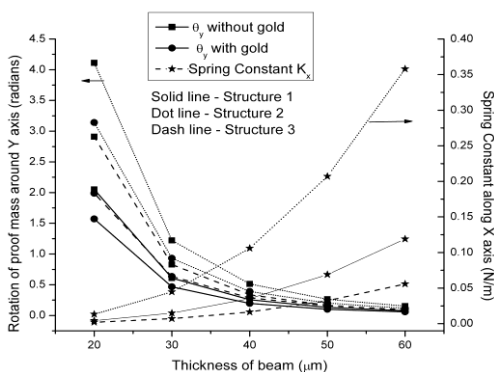


**Fig-9:** Variation of rotational cross axis sensitivity of proof mass and spring constant for X axis acceleration with thickness of the beam

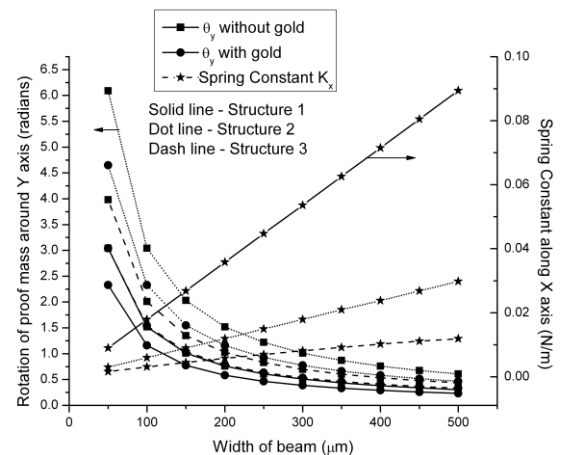


**Fig-10:** Variation of rotational cross axis sensitivity of proof mass and spring constant for X axis acceleration with width of the beam

In the case of multiple suspended beam configurations where the beams are positioned at the edges of the proof mass, when thickness of the beam is varied from 10 $\mu\text{m}$  to 60 $\mu\text{m}$ , there is percentage reduction in cross axis sensitivity from 23.42% to 23.65% for the structure with gold as shown in Fig-9. For configuration 2, the percentage decrease in cross axis sensitivity for the structure with electroplated gold is observed is of a constant value of around 23.63%. The percentage reduction in cross axis sensitivity for the structure with electroplated gold was observed to be varying from 23.49% to 31.6% in the case of configuration 3.

As the width of the beam is increased from 50 $\mu\text{m}$  to 500 $\mu\text{m}$ , in configuration 2, there is a percentage reduction in cross axis sensitivity for the structure with gold. The percentage decrease observed is found to be varying from 23.7% to 23.56% as shown in Fig-10. In the case of quad beam configuration where the beams are positioned at the centre on all edges of the proof mass, there is a constant percentage decrease of around 23.64 % in cross axis sensitivity for the structure with gold as the width of the beam is varied. For the quad beam configuration 3 as the width of the beam is increased there is an increase in spring constant while a decrease in cross axis sensitivity is observed. From the graph, we can deduce that there is a percentage decrease in cross axis sensitivity for the structure with electroplated gold which is found to be 23.63%.

### 3. CONCLUSIONS

A comparative study of sensitivity analysis of 3 different accelerometer structures is discussed in this paper. Effect of electroplated gold on these structures has been studied. It can be clearly deduced from the simulation results that configuration 3 where the beams are placed at the corners

of the proof mass has the least cross axis sensitivity around Y axis.

## REFERENCES

[1] Kal S, Ganguly A and Boni A, "An embedded system for pollution control in automobiles by using a MEMS acceleration signal", *Proc. 10th IEEE Int. Conf. on Emerging Technologies and Factory Automation, ETFA (Catania, Italy)*, 2005.

[2] Roushan R T, Saha G, Boni A and Kal, "FPGA implementation of automobile pollution control system using a MEMS accelerometer", *IEEE Int. Conf. Industrial Technology (Mumbai, India)*, 2006.

[3] Roylance L M and Angell J B, "A batch fabricated silicon accelerometer", *IEEE Trans. Electron Devices* **26** 1911-7, 1979.

[5] Pak J J, Kabir A E, Neudeck G W and Logsdon J H, "A bridge-type piezoresistive accelerometer using merged epitaxial lateral overgrowth for thin silicon beam formation", *Sensors Actuators A* **56** 267-71, 1996.

[6] Chen H, Bao M, Zhu H and Shen S, "A piezoresistive accelerometer with a novel vertical beam structure", *Sensors Actuators A* **63** 19-25, 1997.

[7] Sim J-H, Cho C-S, Kim J-S, Lee J-H and Lee J-H, "Eight-beam piezoresistive accelerometer fabricated by using a selective porous-silicon etching method", *Sensors Actuators A* **66** 273-8, 1998.